



The end of the Galactic spectrum

C. DE DONATO¹, G. A. MEDINA-TANCO²

¹*Dipartimento di Fisica dell'Università degli Studi di Milano and INFN, Milano, Italy,*

²*Dep. Altas Energias, Inst. de Ciencias Nucleares, Universidad Nacional Autónoma de México, México DF, CP 04510*

cinzia.dedonato@mi.infn.it

Abstract: We use a diffusion galactic model to analyze the end of the Galactic cosmic ray spectrum and its mixing with the extragalactic cosmic ray flux. We analyze the transition between Galactic and extragalactic components using two different extragalactic models. We compare the sum of the diffusive galactic spectrum and extragalactic spectrum with the available experimental data.

Introduction

The cosmic ray energy spectrum extends for many orders of magnitude with a power law index ≈ 2.7 . Along this range of energies, the three spectral features are known: the first knee at $E \approx 3 \text{ PeV}$, the second knee at $E \approx 0.5 \text{ EeV}$ and the ankle, a dip extending from the second knee to beyond 10 EeV . The nature of the second knee and of the ankle are still uncertain [1]; a possible interpretation of the two features is the transition between the galactic and extragalactic components. At energies between $10^{17} - 10^{18} \text{ eV}$ the galactic supernova remnants (SNRs) are expected to become inefficient as accelerators. This fact, combined with magnetic deconfinement should mark the end of the Galactic component of cosmic rays, although the picture could be confused by the existence of additional Galactic accelerators at higher energy. On the other hand, at energies above the second knee, extragalactic particles are able to travel from the nearest extragalactic sources in less than a Hubble time. Consequently, the spectrum may present above $10^{17.5} \text{ eV}$ a growing extragalactic component that becomes dominant above 10^{19} eV . The region between the second knee and the ankle could be the transition region between the galactic and extragalactic components.

In this work we analyze the transition region comparing the diffusive galactic spectrum from SNRs with two different models of extragalactic spec-

trum, one in which only protons [2] are injected at the sources and another in which a mixed composition containing heavy nuclei [3] is injected.

Diffusion Galactic model

We used the numerical diffusive propagation code GALPROP [4, 5] to reproduce the galactic spectrum from SuperNova Remnants (SNRs). The diffusive model is axisymmetric. The propagation region is, in cylindrical coordinates, bounded by $R = R_h = 30 \text{ kpc}$ and $z = z_h = 4 \text{ kpc}$, beyond which free escape is assumed. The propagation equation is:

$$\frac{\partial \psi}{\partial t} = q(\vec{r}, p) + \vec{\nabla} \cdot (D_{xx} \vec{\nabla} \psi) + \frac{\partial}{\partial p}(\dot{p}\psi) - \frac{1}{\tau_f} \psi - \frac{1}{\tau_r} \psi \quad (1)$$

where $\psi(\vec{r}, p, t)$ is the density per unit of total particle momentum, $q(\vec{r}, p)$ is the source term, D_{xx} is the spatial diffusion coefficient, $\dot{p} = dp/dt$ is the momentum loss rate and τ_f and τ_r are the time scale of fragmentation and the time scale of radioactive decay respectively. The diffusion coefficient is taken as $\beta D_0(\rho/\rho_D)^\delta$, where ρ is the particle rigidity, D_0 is the diffusion coefficient at a reference rigidity ρ_D and $\delta = 0.6$. The distribution of cosmic rays sources used is that of Galactic SNRs

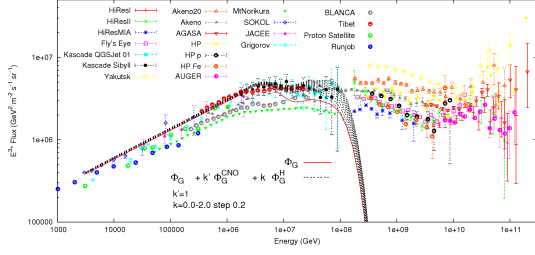


Figure 1: Diffusive Galactic spectrum, Φ_G , with renormalization of the CNO group ($Z:6-12$), Φ_G^{CNO} and of the heavy component ($Z : 19 - 26$), Φ_G^H . Agreement with experimental data is obtained for $k' \approx 1$ and $k \approx 0.8 - 1.2$.

(in agreement with EGRET gamma-ray data) [4]. The injection spectrum is a power law function in rigidity with a break at rigidity ρ_0 , beyond which it falls exponentially with a rigidity scale ρ_c :

$$I(\rho) = \begin{cases} \left(\frac{\rho}{\rho_0}\right)^{-\alpha} & \rho \leq \rho_0 \\ \exp\left[-\left(\frac{\rho}{\rho_0} - 1\right)/\frac{\rho_c}{\rho_0}\right] & \rho > \rho_0 \end{cases}$$

where $\alpha = 2.05$, $\rho_0 = 1.8 PV$ and $\rho_c = 1.26 PV$. Stable nuclei with $Z < 26$ are injected, with energy independent isotopic abundances derived from low energy CR measurements[5].

Detailed and realistic interstellar molecular (H_2), atomic (H) and ionized (HI) hydrogen distributions are used [6].

Diffusive Galactic spectrum

The diffusive galactic spectrum has been normalized to match KASCADE data at $\sim 3 \times 10^6$ GeV. While with this renormalization our spectrum agrees with JACEE and Sokol data at lower energies, beyond the knee the diffusive spectrum presents a strong deficit of flux. Since at $E > 10^7$ GeV the composition is dominated by intermediate ($Z : 6 - 12$) and heavier ($Z : 19 - 26$) nuclei, we renormalize these components by a factor of 2, which produces a good agreement with the experimental data (see Fig. 1).

The renormalized diffusive galactic spectrum reproduces well the data up to $E \approx 10^8 GeV$, be-

yond which the spectrum falls steeply because of end of the SNR acceleration efficiency.

Extragalactic spectrum

In order to study how the transition between the galactic and extragalactic components takes place, we compare the galactic spectrum originated in SNR with two different possible scenarios for the extragalactic component.

In the first model [2], a pure proton extragalactic spectrum, accelerated by a homogeneous distribution of cosmic sources, is considered. Local overdensities/deficits of UHECR sources affect the shape of the GZK modulation, but do not affect the low energy region where the matching with the Galactic spectrum occurs. Different cases of local overdensity/deficiency of sources are considered within this model.

In the second model [3], the extragalactic spectrum is calculated for a mixed composition at injection typical of low energy cosmic rays for different source evolution models in red shift.

In both cases, the various parameters of the models are tuned to fit the available CR data at UHE and are, in that highest energy regime, experimentally indistinguishable at present.

Combined spectrum: matching Galactic and extragalactic components

In order to study how the transition between the Galactic and extragalactic components takes place, we subtract the combined theoretical (Galactic plus extragalactic) spectrum from the available data. Two different approaches are used.

First, we try to match the experimental data by varying the normalization of the heavy Galactic component, while keeping constant the previous renormalization of the CNO group. The best reproduced spectrum for the two extragalactic models are shown in Figs.2, 3 and 4. In the case of the *proton* model, a discontinuity appears when the two spectra are added, regardless of the lower limit adopted for the extragalactic component: 10^8 GeV (Fig.2) or 5×10^7 GeV (Fig.3). The latter cor-

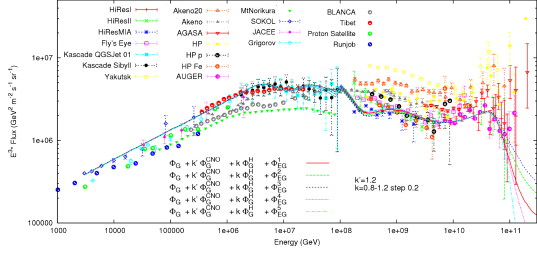


Figure 2: Galactic and Extragalactic spectrum matching for the *proton* models for a EG lower energy limit of 10^8 GeV. The sum of the renormalized diffusive Galactic spectrum and different extragalactic spectrum models (Φ_{EG}) is shown for different renormalizations of the heavy component (Φ_G^H). The CNO group (Φ_G^{CNO}) of the diffusive Galactic spectrum (Φ_G) has been renormalized by a factor 2.2. Different cases of local overdensity/deficit of sources are considered [2]: (1) universal spectrum, (2) and (3) overdensity of sources, (4) and (5) deficit of sources .

responds to cosmic accelerators operating for the entire Hubble time.

For both, *proton* and *mixed-composition* models, there is a flux deficit above 10^8 GeV. The problem is much stronger for the *mixed-composition* model where, regardless of the luminosity evolution of EG CR sources, the total spectrum presents a large deficit of flux between 10^8 and $\approx 3 \times 10^9$ GeV (Fig.4).

In order to solve this flux deficit, the only way out seems to be the introduction of an additional Galactic component. We estimate this component

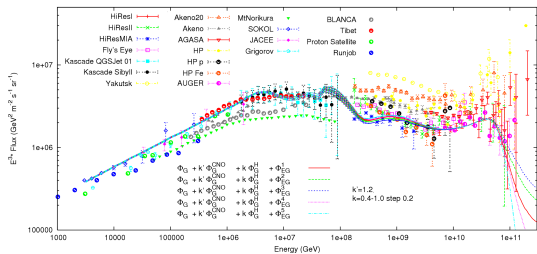


Figure 3: Idem to Fig. 2 but for the *proton* model with a lower energy limit of 5×10^7 GeV.

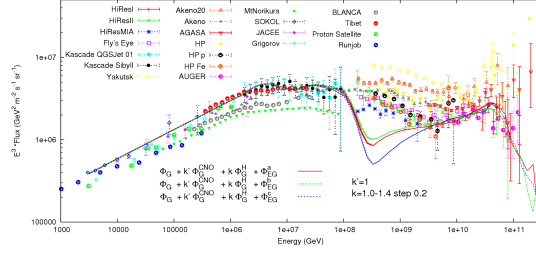


Figure 4: Idem to Fig.3 but for the Galactic and Extragalactic spectrum for the *mixed-composition* model. The CNO group (Φ_G^{CNO}) of the diffusive Galactic spectrum (Φ_G) has been renormalized by a factor 2. Three source evolution models are considered [3]: (a) strong, (b) SFR and (c) uniform.

by subtracting the sum of the diffusive Galactic and extragalactic fluxes from a smooth fit to the world data. This method confirms us the need of the renormalization of the CNO group by a factor ≈ 2.2 and ≈ 2 for the *proton* and *mixed-composition* models, respectively. In the case of the *proton* models (Figs.5, 6), the observed deficit can be resolved with an additional heavy component, while in the *mixed-composition* models this is not enough and we need one more additional heavy component (Fig.7). The additional component common to both families of models is obtained with a shift in energy of a factor ≈ 1.5 of the diffusive galactic heavy component, renormalized by a factor ≈ 0.04 in the case of the *mixed-composition* models and $\lesssim 0.03$ for the *proton* models respectively. The second additional component is obtained in an analogous way but with an energy-shift factor of ≈ 1.8 and a renormalization by a factor 5×10^{-4} . The corresponding spectra are shown in Figs.5, 6 and 7.

Discussion

We have analyzed the matching conditions of the Galactic and extragalactic components of cosmic rays along the second knee and the ankle.

It seems clear that an acceptable matching of the Galactic and extragalactic fluxes can only be achieved if the Galaxy has additional accelerators, besides the regular SNR, operating in the interstel-

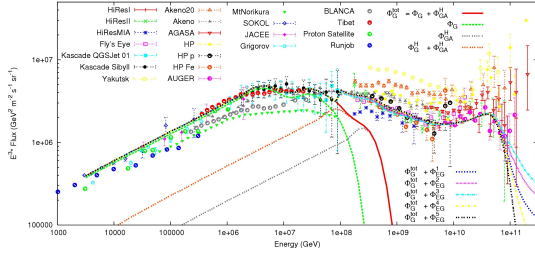


Figure 5: Galactic and Extragalactic spectrum for the *proton* model for an EG lower limit of 10^8 GeV: the additional heavy component ϕ_{GA}^H and the total heavy component ($\phi_G^H + \phi_{GA}^H$) are also shown.

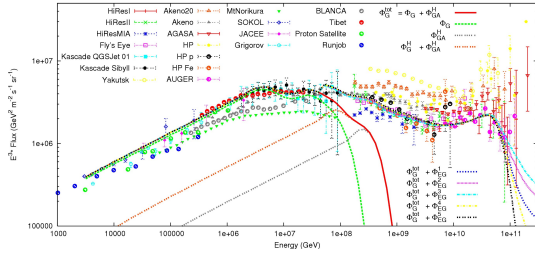


Figure 6: Idem to Fig.5 but for an EG lower limit of 5×10^7 GeV: the additional heavy component ϕ_{GA}^H and the total heavy component ($\phi_G^H + \phi_{GA}^H$) are also shown.

lar medium. In the particular case of the *proton* model, only one additional component is required, and this could well represent the contribution from compact and highly magnetized SNR, like those occurring in the central, high density regions of the Galactic bulge or the dense cores of molecular clouds. It must be noted, however, that a perfectly smooth match seems unrealistic and that some discontinuity, whose magnitude depends mainly on the time depth from which EG CR are able to arrive at our Galaxy, should be eventually observable in the combined spectrum.

The matching of the *mixed-composition* model is more complicated. The Galactic spectrum has to be extended up to the middle of the dip and this requires, besides the previous additional component, another high energy Galactic component. The origin of these cosmic rays pushes even further the

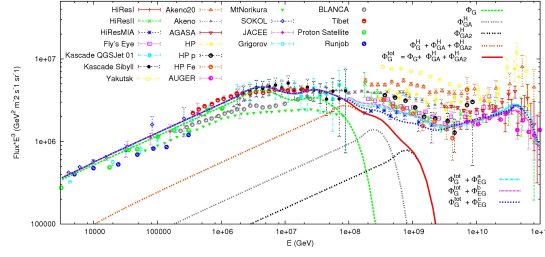


Figure 7: Galactic and Extragalactic spectrum for the *mixed-composition* model: the two additional heavy components ϕ_{GA}^H , ϕ_{GA2}^H and the total heavy component ($\phi_G^H + \phi_{GA}^H + \phi_{GA2}^H$) are shown.

acceleration requirements imposed on the Galaxy and probably rapidly spinning inductors, like neutron stars, could be invoked to fill in the gap. If this were the case, it is very likely that photon emission at TeV energies should uncover the sources. Changes in propagation regime inside the Galaxy at these high energies should manifest as a dipolar anisotropy if enough statistics were available.

Acknowledgements

CDD thanks ICN-UNAM for hosting a long stay and Università degli Studi di Milano for a PhD grant. GMT thanks PAPIIT/CIC-UNAM for support.

References

- [1] G. A. Medina-Tanco, , Proc. EMA 2005, astro-ph/0607543 (2006) 1–34.
- [2] V. Berezhinsky, A. Gazizov, S. Grigorieva, Phys. Rev. D 74 (4) (2006) 043005.
- [3] D. Allard, A. V. Olinto, E. Parizot, , astro-ph/0703633.
- [4] A. W. Strong, I. V. Moskalenko, ApJ 509 (1998) 212.
- [5] A. W. Strong, I. V. Moskalenko, http://galprop.stanford.edu/web_galprop/galprop_home.html, Adv. Sp. Res. 27 (2001) 717.
- [6] I. V. Moskalenko, A. W. Strong, J. F. Ormes, M. S. Potgieter, ApJ 565 (2002) 280.